

# A model-based sustainable productivity concept for the best decision-making in rough milling operations

G. Urbikain Pelayo<sup>a,\*</sup>, D. Olvera-Trejo<sup>b</sup>, M. Luo<sup>c</sup>, K. Tang<sup>d</sup>, L.N. López de Lacalle<sup>a</sup>,  
A. Elías-Zuñiga<sup>b</sup>

<sup>a</sup> University of the Basque Country, UPV/EHU, Aeronautics Advanced Manufacturing Center CFAA, Bizkaia Science and Technology Park, 202, Zamudio 48170, Spain

<sup>b</sup> Tecnológico de Monterrey, Escuela de Ingeniería y Ciencias, Av. Eugenio Garza Sada 2501, Monterrey, Nuevo León 64849, Mexico

<sup>c</sup> Key Laboratory of High Performance Manufacturing for Aero Engine (Northwestern Polytechnical University), Ministry of Industry and Information Technology, Xi'an, PR China

<sup>d</sup> Hong Kong University of Science and Technology, Hong Kong, China

## ARTICLE INFO

### Keywords:

Productivity  
Sustainability  
Rough milling  
Power consumption  
Force models

## ABSTRACT

There is a need in manufacturing as in machining of being more productive. However, at the same time, workshops are also urged for lesser energy waste in cutting operations. Specially, rough milling of impellers and bladed integrated disks of aircraft engines need an efficient use of energy due to the long cycle times. Indeed, to avoid dramatic tool failures and idle times, cutting conditions and operations tend to be very conservative. This is a multivariable problem, where process engineers need to handle several aspects such as milling operation type, toolpath strategies, cutting conditions, or clamping systems. There is no criterion embracing productivity and power consumption.

In this sense, this work proposes a methodology that meets productivity and sustainability by using a specific cutting energy or sustainable productivity gain (SPG) factor. Three rough milling operations -slot, plunge and trochoidal milling- were modelled and verified. A bottom-up approach based on data from developed mechanistic force models evaluated and compared different alternatives for making a slot, which is a common operation in that kind of workpieces. Experimental data confirmed that serrated end milling with the highest SPG value of 1 is the best milling operation in terms of power consumption and mass removal rate (MRR). In the case of plunge milling technique achieve an  $SPG < 0.51$  while trochoidal milling produces a very low SPG value.

## 1. Introduction

Metalworking companies are constraint to satisfy international standards for selling goods in very competitive markets. Meanwhile, climate change and air pollution are pushing for urgent solutions and mindset changes. In recent years, the need for efficient use of energy was demonstrated to be an imperative goal [1]. The machining of impellers and bladed integrated disks (blisks) of aircraft engines reflects this paradox. On the other hand, the fleet of active engines will increase by 18,000 units [2] during the next decade. According to this study, in 2026 more than half of the engine fleet will be replaced by new-generation models. These numbers give an idea of what we shall expect also from manufacturing processes: productivity with sustainability.

Because of their high-added value, the use of conservative cutting parameters in the machining of aerospace parts is a usual trend in the workshop. This *modus operandi* tends to increase cycle times and power consumption. To reduce cutting forces and power, innovative ideas are continuously drawn by toolmakers. For instance, to get a different engagement between tool and workpiece, new approaches can be divided into two important groups: 1) design of complex tools (geometry); 2) use of alternative milling kinematics. These solutions are combined with a planned CAM strategy (NX®, Hypermill®, etc.) for efficient use of cutting parameters and machine tool's linear axes.

Focusing on the first group, innovative cutting tools have been designed and modelled for an efficient chip removal rate. Toolmakers created new geometries for solid mills (variable pitch/helix tools, serrated end mills, etc.) as for indexable milling tools (porcupine tools,

\* Corresponding author at: University of the Basque Country, Aeronautics Advanced Manufacturing Centre, Plaza Europa 1, Donostia-San Sebastián ZIP code: 20018, Spain.

E-mail addresses: [gorka.urbikain@ehu.es](mailto:gorka.urbikain@ehu.es) (G. Urbikain Pelayo), [daniel.olvera.trejo@tec.mx](mailto:daniel.olvera.trejo@tec.mx) (D. Olvera-Trejo), [luoming@nwpu.edu.cn](mailto:luoming@nwpu.edu.cn) (M. Luo), [mektang@ust.hk](mailto:mektang@ust.hk) (K. Tang), [norberto.lzlacalle@ehu.eus](mailto:norberto.lzlacalle@ehu.eus) (L.N. López de Lacalle), [aelias@tec.mx](mailto:aelias@tec.mx) (A. Elías-Zuñiga).

<https://doi.org/10.1016/j.measurement.2021.110120>

Received 23 June 2021; Received in revised form 18 August 2021; Accepted 28 August 2021

Available online 8 September 2021

0263-2241/© 2021 The Author(s). Published by Elsevier Ltd. This is an open access article under the CC BY license (<http://creativecommons.org/licenses/by/4.0/>).

**Nomenclature**

$A$	Sinusoidal wave amplitude	$P_0$	Idle power
$a_e$ [mm]	Radial depth of cut	$P$	Cutting power
$a_p$ [mm]	Axial depth of cut	$Q_w$ [mm <sup>3</sup> /s]	Chip flow
$c$ [mm]	Stepover (orbit)	$R_a$ [μm]	Surface roughness
$D$ [mm]	Tool diameter	$r_{orb}$	Orbit radius
$D_s$	Width of the slot	$N$ [rpm]	Spindle speed
$d_{orb}$	Orbit diameter	$t$ [s]	Total cutting time
$dF_{x,y,z}$ [N]	Differential Force component in x-, y- and z-axis	$t_1$ [s]	Cutting period
$F_c$	Resultant cutting force	$t_2$ [s]	Idle period
$F_{t,r,a}$ [N]	Force in tangential, radial and axial directions	$v_f$ [mm/rev]	Feed per revolution
$F_{x,y,z}$ [N]	Force component in x-, y- and z- axis	$v_r$ [mm/min]	Linear feed
$f_z$ [mm/Z]	Feed per tooth	$V$ [mm <sup>3</sup> ]	Removed volume
$K_{tc}, K_{rc}, K_{ac}$ [N/mm <sup>2</sup> ]	Shear Cutting coefficients in tangential, radial and axial directions	$V_c$ [m/min]	Cutting speed
$K_{te}, K_{re}, K_{ae}$ [N/mm]	Edge Cutting coefficients in tangential, radial and axial directions	$Z$ [-]	Number of flutes
		$\beta$ [°]	Helix angle
		$\lambda$	Wavelength period of sinusoidal wave
		$\kappa$ [°]	Side cutting edge angle

high-feed inserts, etc.). Variable helix and pitch cutters were proved to reduce the tendency to chatter and cutting vibrations [3–5]. Serrated end mills, based on wavy -sinusoidal or trapezoidal- cutting-edge profiles, also positively affect cutting forces. Koca et al. [6] studied the effect of the serration parameters (wavelength period and amplitude) on the boundary limits. Grabowski et al. [7] used the semi-discretization method to study chatter using different axial locations of the engaged depth of cut. Tehranizadeh et al. [8] gave a complete perspective of static and dynamic forces proving that these tools can improve stability margins. Recently, Urbikain and Olvera [9] detailed a new approached for keeping a compromise between forces and surface finish. These authors optimized the phase shift angle between flutes to satisfy both requirements: minimum forces and surface accuracy.

On side of process kinematics, alternative strategies to conventional milling can be applied for a more efficient mass removal rate (MRR). First, the plunge milling process can be a promising alternative. In this case, the tool is fed along tool axis  $z$  (or spindle axis), which is far more rigid than  $x$ - $y$  directions. So, it is appropriate for operations where a high mass removal rate (MRR) is desired and the tool travels large depths, such as cavities. Ko and Altintas [10] described the basis of plunge milling operations by proposing a time-domain model. They considered the chip regeneration mechanism to study torsional-axial vibrations and validated their model through experimental tests. Zhuang et al. [11] studied plunge milling stability while machining difficult-to-cut materials. These authors employed (and validated) the frequency-domain method for an efficient, chatter-free, chip removal through the optimization of radial cutting widths. Yang and Tang [12] studied the feasibility of plunge milling for face-gear machining and proved its advantages. These authors approached the problem from a theoretical (geometrical) point of view using Vericut software. Han et al. [13] applied multi-axis plunge milling for the rough machining of impeller parts. They formulated the interaction between the cutter and workpiece and demonstrated that an efficient optimization of some elements - tool length, cavity depth, tool inclination angles and overlap distance between passes - can improve time cycles up to 40%. More lately, Cafieri et al. [14] focused on controlling cutting parameters via machine tool's CNC online. They determined optimal values through continuous variation: cutting speed, feed rate and overlap between passes. Secondly, trochoidal milling emerges as a faster and more productive chip evacuation technique than conventional milling. It is applied to slot and pocket milling applications. Otkur and Lazoglu [15] gave a pioneering analysis of trochoidal milling developing a numerical engagement model and even proposing a second strategy: the double trochoidal milling. Both models were validated with experimental tests in

aluminum alloy Al7039. Due to its efficiency in mass removal rate, some authors studied this technique for the milling of pockets and cavities to save surface finish at the corner where the tool's load is higher. Wu et al. [16] successfully applied a control strategy for cavity trochoidal milling that reduced vibrations and tool wear. Pleta et al. [17] studied via Taguchi method the relationship between input (model) and output (force and wear) parameters. These authors investigated the effects of the trochoidal path and tool wear on the region beneath the machined surface. Some authors analyzed in depth the problem and studied its kinematics with further axes. Luo et al. [18] proposed a four-axis trochoidal toolpath using a ball-end mill for the machining of blisk channels. The trochoidal paths were raised in parametric domain and controlled to produce smooth orientations and movements. The method can be expanded to five-axis milling. Li et al. [19] proposed an original approach to maximize mass removal rate (MRR) in the trochoidal milling of cavities by generating a spatial cubic curve-based cyclic five-axis tool path.

The problem of energy consumption in milling centers was also faced through modelling. Avram and Xirouchakis [20] evaluated the energy requirements of the spindle and linear axes in a milling operation. Their methodology was experimentally verified considering both steady-state and transient regimes. In a conceptual work, Balogun and Mativenga [21] showed the influence of several machine components (state power, tool change, air cutting power) on power and energy consumption for a machine tool. Sealy et al. [22] proposed an interesting approach by linking cutting specific energy to surface integrity. They demonstrated that specific energy is a valuable indicator for process signature and can give the path to surface integrity control. Ma et al. [23] proposed a specific energy calculation model to predict the electrical energy consumed by a three-axis milling machine, and optimized focused on controlling spindle speed. Xu et al. [24] investigated the problem of energy consumption in five-axis operations. They proposed an algebraic-based model to find an equilibrium between energy consumption and the desired toolpath. They obtained savings of 25% in the consumed energy. Lv et al. [25] proposed a model to estimate power and energy consumption of spindle acceleration in a CNC lathe. They found very close results between simulation and experiments data (<6%). Shin et al. [26] used *component-models* to predict energy consumption as a function of machining setup, cutting parameters, and real-time monitoring data that were handled to retrofit the model. Wojciechowski et al. [27] presented a multi-criteria optimization method focusing on force reduction which is an indicator of power consumption. They applied the response surface method to improve ball-milling operations in inclined surfaces. Cai et al. [28,29] developed a method for the identification of

energy efficiency state. Continuous wavelet transform was combined with Fast independent component analysis and Hidden Markov model. Later, Shi et al. [30] developed an energy prediction model, but considering the effects of tool wear. These authors claimed that it could be inversely used for tool wear estimation. Later, the same research group refined the method and found more accurate results [31]. They verified their improved model in Aluminum and Titanium alloys. However, that work only focused in common milling operations -slot and peripheral milling. Venkata Rao [32] proposed a teaching learning-based optimization technique coupled with FEM simulation to obtain the best cutting parameters combination in micro-milling of D2 steel. As a result, cutting forces and power as well as residual stresses were reduced. Zhang et al. [33] proposed a complete mechanical milling power model and then validated it through experimental tests. They found feed parameter is the most important cutting parameter when it comes to improving mass removal rate. Recently, with the aim of extracting key frequency features in the cutting signal, Yuan et al. [34] developed and applied some numerical algorithms. The outcomes give a clue for intelligent monitoring and maintenance. Nevertheless, additional studies need to be done for implementation in industrial practice. Nguyen [35] proposed an multi-parameter optimization of machining energy. In that work, specific cutting energy, material removal rate, and roughness were optimized simultaneously using Kriging models.

Cutting force and power prediction is a hot topic in machining [36,37]. However, despite both magnitudes are connected, works in the literature tend to study them under different approaches. On one hand, force models can be occupied by authors who face the problem from a physico-mechanical point of view. Such research groups also tend to study collateral, neighboring problems such as surface roughness [38–41], vibrations [42–45] or tool wear [46]. On the other hand, cutting power models are most of times developed from purely empirical approaches, profiting from the fact that power is a simple, scalar and significant value in machining.

From the above, some gaps are identified. First, power models are very often considered from a statistical or empirical point of view, handling enormous data that are retrofitted towards an empirical model. In that cases, the meaningfulness of cutting theory and mechanics for energy calculation tends to be left out of the problem. Second, to the authors' knowledge, there is no attempt in the literature of characterizing productivity including at the same time sustainability criteria in machining operations. Very often, works dealing with forces and power in machining processes try to maximize or minimize one single aspect. For instance, minimizing cutting power (or cutting forces) or maximize productivity. Third, models lack of generality as tend to be verified on quite specific cutting operations.

There is an obvious conflict between productivity and energy consumption because being productive is often associated with an increase in the cutting power requirements. In particular, at the rough stage there is a margin for improvement. Besides, choosing the best milling process and cutting conditions is also a challenge. This paper presents a bottom-up approach for the decision-making during the definition of rough milling process that meets both, productivity and sustainability. Here, a selection criterion is proposed. It is based on the information from mechanistic force models. A sustainable productivity gain (SPG) factor enables qualifying any given pair of operation datasets considering both aspects. As proof of concept, different processes -plunge milling, trochoidal milling and serrated milling- were measured and evaluated as alternative processes for a typical rough milling operation. First, Section 2 depicts the methodology throughout the work. Section 3 presents the kinematics and tool specifications for the different milling processes. Section 4 and 5 (level 0-1-2) illustrate the basis for force modelling and the validation of these models respectively. Section 6 proposes a new index, the Sustainable Productivity Gain (SPG) to select the most efficient alternative having in mind both productivity and energy preservation. Finally, some conclusions are drawn.

## 2. Methodology

At the rough stage, productivity is constraint by conservative cutting parameters resulting in long, time-consuming operations and resulting in a waste of energy. In the practice, there are many different scenarios (milling alternatives, tool features, cutting parameters) and there is not an objective-quantitative criterion to choose one above another. Machinists and even process engineers tend to follow rules based on their expertise, recommendations from toolmakers, etc. This is not enough if aiming for improved and cleaner processes.

Fig. 1 shows the workflow diagram used to improve the decision-making process at that stage. Level 0 represents almost an instantaneous first step in the procedure. Chip flow can be calculated as an indicator of mass removal rate and process productivity. Then, level 1 attempts to develop and validate the models in terms of the predicted milling forces. Output parameters can be representative features regarding cutting forces: mean, maximum and peak to peak values. Here, input parameters are 1) milling type or kinematics (plunge, trochoidal, serrated); 2) tool geometry (solid end mill or replaceable inserts, tool diameter  $D$ , helix angle  $\beta$ , tooth number  $Z$ , side cutting edge angle  $\kappa$ , amplitude  $A$  and wavelength  $\lambda$ ); 3) cutting parameters: axial depth of cut  $a_p$ , radial depth of cut  $a_e$ , feed  $f_z$  and spindle speed  $N$  (or cutting speed  $V_c$ ). Subsequently, the developed models are upgraded to the highest level 2. Once fixed the geometry of the operation, milling strategy and cutting parameters, the models generate higher degree output parameters to qualify the alternatives from the point of view of productivity and energetic efficiency: removed chip volume/time and power consumption. Alternatively, practitioners could measure both, cutting forces (more expensive, using dynamometers) as cutting power (cheaper, using power meters). In this work, we will check both approaches: modelling and experimentation.

## 3. Alternatives for rough milling

Slot milling is a common strategy for roughing because it combines a high chip removal rate with the simplest tool trajectory. However, milling tools put through high stress due to the big interference between tool-workpiece. Cutting forces tend to be very high and so, deep grooves often require several longitudinal passes and reduce the total depth of cut into smaller steps.

Slot milling operation can be done in a 3-axis machining center (as will be the case here) but finds its maximum operability in 4- and 5-axis to prepare complex surfaces in bladed disks and impellers. It is used as an initial cutting strategy with the usual patterns of zigzag trajectories. In these cases, the intersections with the geometry at certain levels are taken as a reference, to generate the curved paths between the blades. Typically, these levels are surfaces parallel to one of the surfaces of revolution of the piece (hub/shroud) or interpolation between the two. Bearing in mind this reference operation, Fig. 2 presents the different milling processes and their main features.

It is observed how heterogeneous the many available solutions can be. As a reference system, the  $x$ -axis is taken as the longitudinal direction of the slot while the  $z$ -axis represents tool axis direction, the  $y$ -axis is the counterfeed (normal) direction. From the selected processes, serrated and plunge milling use a tool with the same diameter as the slot, while trochoidal milling strictly needs a smaller tool ( $D < a_e$ ), enabling trochoidal trajectories. Besides, its process kinematics is more complicated: there are up to 5 parameters and feed direction continuously changes in  $x$ - $y$  plane. On the other hand, the concept of axial depth of cut disappears for plunge milling. So, the decision of choosing the best alternative could be not so clear and straightforward.

Serrated milling can be a good solution for slot milling operations due to its relatively low cutting forces in comparison with conventional straight (cylindrical) cutting tools. Serrated tools present a sinusoidal geometry along the tool helix, causing a variation in the tool radius, in the side cutting edge angle and so, leading to a varying work/tool

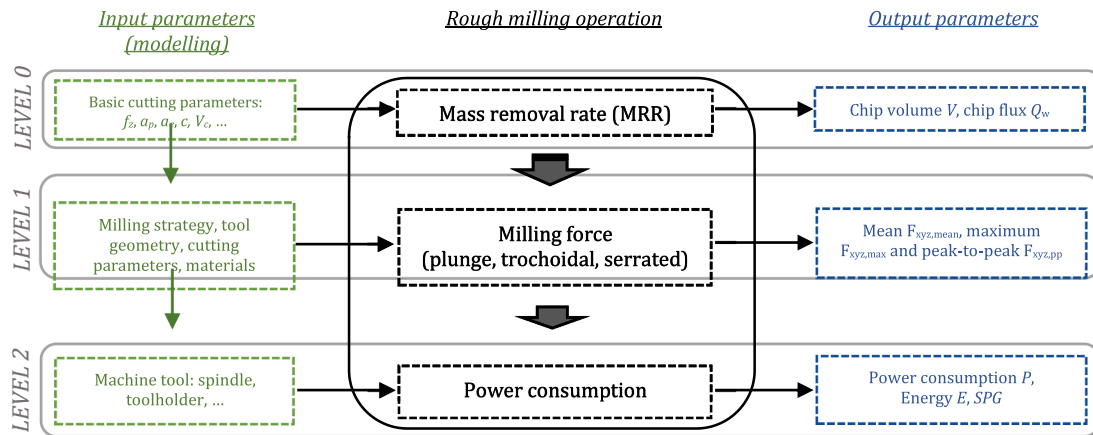


Fig. 1. Workflow diagram to evaluate efficient rough milling operations.

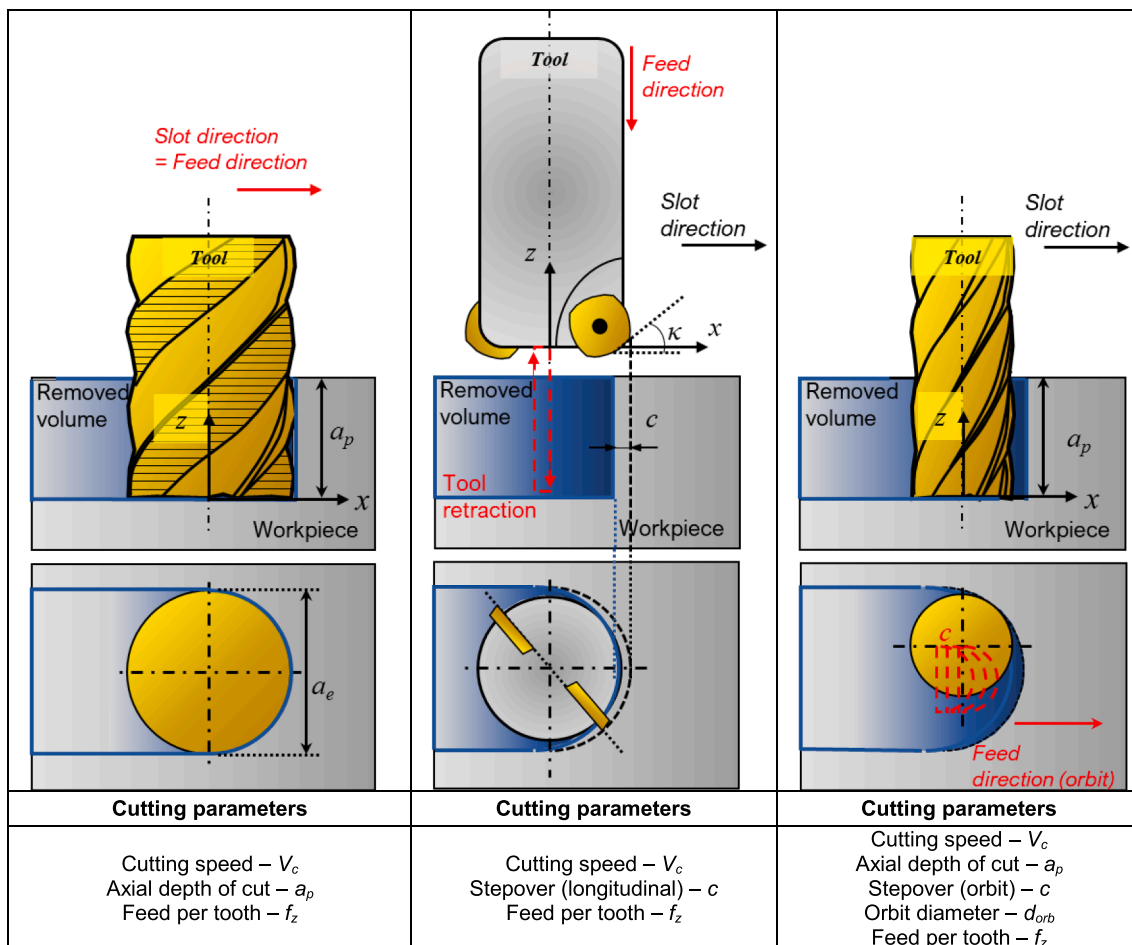


Fig. 2. Slot milling alternatives. A. Serrated milling; b. Plunge milling; c. Trochoidal milling.

contact time along the direction of the depth of cut. Besides tool diameter  $D$  and helix angle  $\beta$ , two additional geometric parameters need to be defined: the amplitude  $A$  and wavelength period  $\lambda$  of the sculptured sinusoidal wave. Side cutting edge angle is measured as the angle contained between the cutting edge and the horizontal plane. Besides, plunge milling and trochoidal milling are studied as possible candidates. In plunge milling, the feed or penetration movement is done in the tool axis direction  $z$  so the expected predominant cutting force component is  $F_z$ . It is a valid alternative when peripheral milling would lead to

excessive vibrations, i.e., when using long tool overhangs, or when milling low machinability materials (such as titanium or nickel alloys). This aggressive milling is done with the theoretically secondary cutting edge of the milling cutter, instead of using the main cutting edge. To avoid excessive cutting forces the overlap between passes must be controlled. Trochoidal milling is an effective way of removing material for machine tools with enough dynamic capabilities. Trochoidal kinematics is based on programming circular paths to keep a smaller engaged (tool/work) contact angle. As a result, lower cutting forces and

tool wear are expected. However, the design and generation of trochoidal trajectories are more complex than programming plunge milling. For high depths, the slot is divided into several axial passes.

In milling, two different reference systems need to be defined. A local one, moving with the tool,  $t$ - $r$ - $a$  ( $t$  = tangential,  $r$  = radial,  $a$  = axial), and a fixed one,  $xyz$  (where  $xy$  is the horizontal plane and  $z$  overlaps with tool axis),  $x$  is the longitudinal direction of the slot. So, the tangential cutting force  $F_t$  is in the direction of cutting speed, the axial force  $F_a$  is parallel to the cutting-edge direction, while  $F_r$  takes place along the orthogonal direction to the cutting edge. For trochoidal milling, the variation of  $F_x$  and  $F_y$  is quite similar but shifted due to the circular path. This process leads to the lowest  $F_z$  component. Even different between processes, plunge and trochoidal milling give comparable  $F_x$  and  $F_y$  forces, while  $F_y$  force component is predominant in the slot milling with the serrated tool. They also involve a cut-off period of the cutting tool, between subsequent radial passes in the case of plunge or between subsequent orbits in the case of trochoidal milling. The serrated milling process stands as the most aggressive cutting with nonzero values for the three components.

Fig. 3 shows the previously described cutting tools (Hoffmann Garant©), all made of uncoated hard metal (CW). Even if the economical approach is out of scope here, we present their associated costs. First, the serrated tool is the most expensive one: a carbide solid mill, sculptured with a wavy profile over the cutting edge. Then, the most economical alternative, the tool for plunge milling, which is made of *high-feed* indexable inserts. Having  $Z = 2$ , each package of 10 items enables replacing them up to 5 times. Finally, the trochoidal tool, which is not very much different than a conventional straight solid end mill, but specially prepared for suffering high axial depths of cut.

#### 4. Milling force models for the candidate processes

Milling force models can predict cutting forces with relatively high accuracy under a range of cutting conditions. Mechanistic force models assume a proportionality relationship between the local forces acting on the rotating tool and the chip thickness. These differential cutting forces are generally written in the local system  $t$ - $r$ - $a$  as:

$$\begin{aligned} dF_{tj}(\phi_j, z) &= g(\phi_j) \cdot [K_{t,c} h(\phi_j, z) dz + K_{t,e} dz] \\ dF_{rj}(\phi_j, z) &= g(\phi_j) \cdot [K_{r,c} h(\phi_j, z) dz + K_{r,e} dz] \\ dF_{aj}(\phi_j, z) &= g(\phi_j) \cdot [K_{a,c} h(\phi_j, z) dz + K_{a,e} dz] \end{aligned} \quad (1)$$

where  $g(\phi_j)$  is a function that detects whether the teeth are engaged in the cut or not,  $h$  is the chip thickness,  $db$  is the differential height element and  $ds$  the differential edge element engaged in the cut.  $K_{tra,c}$  and  $K_{tra,e}$  are the shear cutting coefficients and edge coefficients, respectively, which are calibrated from experimental tests. The cutting forces in Eq.1 need to be integrated along with the full axial depth of cut, summed for all the teeth engaged in the cut and projected over the directions of the inertial frame of reference.

Serrated and trochoidal models are here described using shear and friction components while plunge milling was simplified through shear cutting coefficients. Table 1 raises the main parameters in the identification of cutting forces. Among all these parameters, the chip thickness is a mandatory variable for the numerical computation of cutting forces. It can be difficult to find in a closed-form expression for some milling operations. Regarding the side cutting edge angle, it is constant for straight cutting tools (trochoidal) and can be assumed as constant for high-feed plunge milling, while it is variable along with the sinusoidal wave for serrated end-mills. Some other assumptions of the models are: 1) no runout effects were considered; 2) rigid cutting conditions (no chatter).


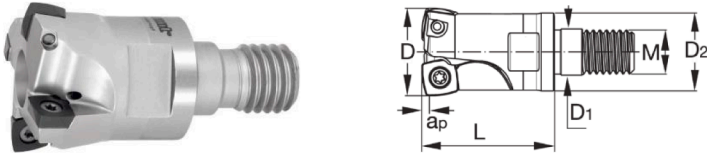

Cutting process	Cutting tools				
Serrated milling (sinusoidal solid end mill) Cost: 220.80 €					
	Tool diameter D [mm]	Flutes Z [-]	Helix angle [°]	Maximum cutting length [mm]	Material
	20	3	45	60 mm	Uncoated WC (MDI)
Plunge milling (replaceable inserts) Cost: 135.10 € (10 inserts)					
	Tool diameter D [mm]	Flutes Z [-]	Helix angle $\beta$ [°]	Maximum cutting length [mm]	Material
	20	2	[-]	0.85	Uncoated WC
Trochoidal milling (solid end mill) Cost: 125.00 €					
	Tool diameter D [mm]	Flutes Z [-]	Helix angle [°]	Maximum cutting length [mm]	Material
	12	3	45	61 mm	Uncoated WC

Fig. 3. Cutting tools and geometrical data.



**Table 1**  
Differential forces in xyz system for the three candidate processes.

Candidate processes	Absolute differential cutting forces $dF_x, dF_y, dF_z$
Serrated milling [9]	$dF_{x,j} = \cos\phi_j \cdot dF_{t,j} + \sin\phi_j \sin\kappa_{zR} \cdot dF_{r,j} - \sin\phi_j \cos\kappa_{zR} \cdot dF_{a,j}$ $dF_{y,j} = -\sin\phi_j \cdot dF_{t,j} + \cos\phi_j \sin\kappa_{zR} \cdot dF_{r,j} - \cos\phi_j \cos\kappa_{zR} \cdot dF_{a,j}$ $dF_{z,j} = -\cos\kappa_{zR}(j, z) \cdot dF_{r,j} + \sin\kappa_{zR} \cdot dF_{a,j}$
Plunge milling [10]	$dF_{x,j} = -\cos\phi_j \cdot dF_{t,j} + \sin\phi_j \sin\kappa \cdot dF_{a,j} - \sin\phi_j \cos\kappa \cdot dF_{r,j}$ $dF_{y,j} = \sin\phi_j \cdot dF_{t,j} + \cos\phi_j \sin\kappa \cdot dF_{a,j} - \cos\phi_j \cos\kappa \cdot dF_{r,j}$ $dF_{z,j} = -\cos\kappa(j, z) \cdot dF_{a,j} - \sin\kappa \cdot dF_{r,j}$
Trochoidal milling [15]	$dF_{x,j} = \cos\phi_j \cdot dF_{t,j} + \sin\phi_j \cdot dF_{r,j}$ $dF_{y,j} = -\sin\phi_j \cdot dF_{t,j} + \cos\phi_j \cdot dF_{r,j}$ $dF_{z,j} = dF_{a,j}$

## 5. Simulations and experimental validations

This section presents the bottom-up approach aiming for a descriptor of milling operation: the sustainable productivity gain. As mentioned, the approach is divided into 3 different levels.

### 5.1. Level 0: Chip flow calculation

For plunge milling operation, the classical formula for chip flow ( $Q_w = V/t = a_p \cdot D \cdot L/t$ , where  $V$  is the removed volume and  $t$  the total time) for the whole operation is verified against a computed value taking into account the programmed toolpath. For a single pass, the chip flow should also satisfy:

$$Q_w = \frac{V}{t} = \frac{c \cdot D \cdot a_p}{t_1 + t_2} \quad (2)$$

where  $a_p = 60$  mm is the height of the slot,  $c$  is the slope between vertical passes,  $D$  is tool diameter,  $t_1$  and  $t_2$  stand for the cutting and idle periods. If using, as usual, the work feed rate during machining (G1) and the maximum feed (G0) during tool retraction and considering than during retraction the tool goes to  $X = -0.5$  and  $Z = +0.5$  and then to  $X$  (safety plane):

$$t_1 = \frac{a_p}{v_{f,1}} \quad (3a)$$

$$t_2 = \frac{\sqrt{\left((a_p + 0.5)^2 + 0.5^2\right)} + 0.5 + 0.5}{v_{f,2}} \quad (3b)$$

where  $v_{f,1} = f_z \cdot Z \cdot N$  and  $v_{f,2} = f_{z,max} \cdot Z \cdot N$  (with  $Z = 2$ ,  $N = 2,800$  rpm and  $f_{z,max} = 0.578$  mm/Z/rev).

Similarly, chip flow is computed for trochoidal milling as:

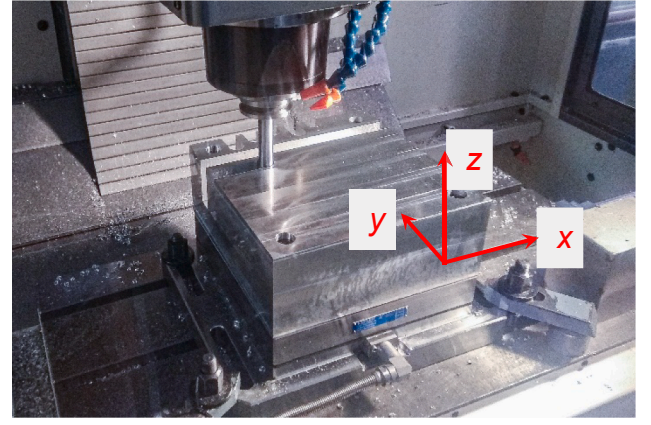
$$Q_w = \frac{V}{t} = \frac{c \cdot D_s \cdot a_p}{t_1 + t_2} \quad (4)$$

where  $a_p = 60$  mm is the height of the slot,  $c$  is the slope between the planetary orbits,  $D_s$  is the width of the slot ( $D_s = 20$ ),  $t_1$  and  $t_2$  stand for the cutting and idle periods. In this case,  $t_2$  was also programmed using the work feed rate (G1). So, the time for a single pass considering that the effective machining is done during  $1/2$  of the orbit:

$$t = t_1 + t_2 = \frac{s_1}{f_z \cdot Z \cdot N} + \frac{s_2}{f_z \cdot Z \cdot N} = \frac{\pi r_{orb} + s_2}{f_z \cdot Z \cdot N} \quad (5)$$

where  $r_{orb} = 0.5 \cdot (D_s - D) = 0.5 \cdot (20 - 12) = 4$  mm is the orbit radius and  $s_2 = 25.62$  mm is the length during tool retraction.

For serrated milling, the calculation of machining time and chip flow is straightforward as there are no idle times. The tool is in permanent contact with the workpiece through the pass and the feed is linear along the x-axis (see Fig. 4). So, for serrated milling-as for slot milling- it is computed as:



**Fig. 4.** Example of slot milling operation using plunge strategy and Kistler's axes.

$$Q_w = \frac{V}{t} = \frac{a_p \cdot a_e \cdot v_f}{t} \quad (6)$$

We will refer again to these values in Table 6.

### 5.2. Level 1: Cutting forces

In order to validate the proposed methodology, first, the cutting force models need to be verified. Milling calibration tests were made on an Aluminum (7075 T6) block ( $260 \times 260 \times 100$ ) in a 3-axis machining center (Kondia B640). Kistler 3-component dynamometer (9257B) and charge amplifier were used to measure the cutting forces (see Fig. 4). The x-axis is aligned with the slot direction and feed direction in a common milling operation. The y-axis is the orthogonal direction and the z-axis, as usual, coincides with tool axis direction and feed direction in plunge milling. All the cutting tests were done in wet conditions (conventional oil emulsion). Starting cutting conditions were based on toolmakers' recommendations but, to be comparable, some modifications were done. Table 2 shows the main parameters for the characterization tests, where  $a_p$  stands for the axial depth of the slot,  $a_e$  is considered the radial immersion for the serrated tool and  $c$  stands for the stepover in plunge milling or stepover at each planetary orbit in trochoidal milling. From calibration tests, the cutting coefficients were found:  $K_{tc} = 905e6$  [N/m<sup>2</sup>],  $K_{te} = 13e3$  [N/m],  $K_{rc} = 570e6$  [N/m<sup>2</sup>],  $K_{re} = 12e3$  [N/m],  $K_{ac} = 285e6$  [N/m<sup>2</sup>],  $K_{ae} = 1e3$  [N/m].

In order to verify each of the modelled processes, additional experimental studies were conducted. Table 3 shows some of the validations performed for the three tested processes.

Fig. 5 shows the correspondence between the experimental and the simulated forces during five revolutions. A general look at the experimental forces gives a noisier signal for the 3rd channel  $F_z$ . From this section, serrated milling was observed as the most productive process (higher mass removal rates) but attention must be paid to the power consumption. In the case of plunge milling (Fig. 5b), the cutting force pattern is repeated every  $180^\circ$  in a two flutes cutter and a small runoff effect is seen in the experimental cutting forces. Even if the z-axis is in a very sensitive direction, a favorable shape and equilibrium between the three components can be maintained if the radial slope between passes is kept under control. In all the cases, the relative error between predicted peaks (maximum force components) and experimental ones is below 13%. A good estimation is obtained from models even not considering tool's runoff.

### 5.3. Level 2: Power and energy

In sub-heading 5.2, Level 1 accomplished the task of force models development and validation. As explained before, the most efficient

**Table 2**

Cutting parameters for the characterization tests.

Cutting process	$a_p$ [mm]	$a_e$ or $c$ [mm]	$f_z$ [mm/rev/tooth]	$v_f$ [mm/min]	$N$ [rpm]	$V_c$ [m/min]
Serrated milling	10	20	0.10–0.15–0.20	1074–1611–2149	3,581	225
Plunge milling	70	1.25–1.5–1.75	0.15–0.175–0.20	840–980–1120	2,800	176
Trochoidal milling	35	0.5–0.75	0.05–0.075–0.1	995–1492–1989	6,631	250

**Table 3**

Cutting parameters for the validation tests (see Fig. 5).

Cutting process	$a_p$ [mm]	$a_e$ or $c$ [mm]	$f_z$ [mm/rev/tooth]	$v_f$ [mm/min]	$N$ [rpm]	$V_c$ [m/min]
Serrated milling	10	20	0.10	1350	4500	282
Plunge milling	60	1.3	0.16	896	2800	176
Trochoidal milling	60	0.8	0.06	1194	6631	250

process here is defined as the one that achieves the best compromise between productivity and power consumption. So, cutting forces, power consumption, removed chip flow will be derived and compared with the experimental values to verify the predictions of the models. Specifically, cutting conditions in Table 4 will be used for the slot milling of a large depth cavity of section 60 mm (height)  $\times$  20 mm (width) with the three candidates.

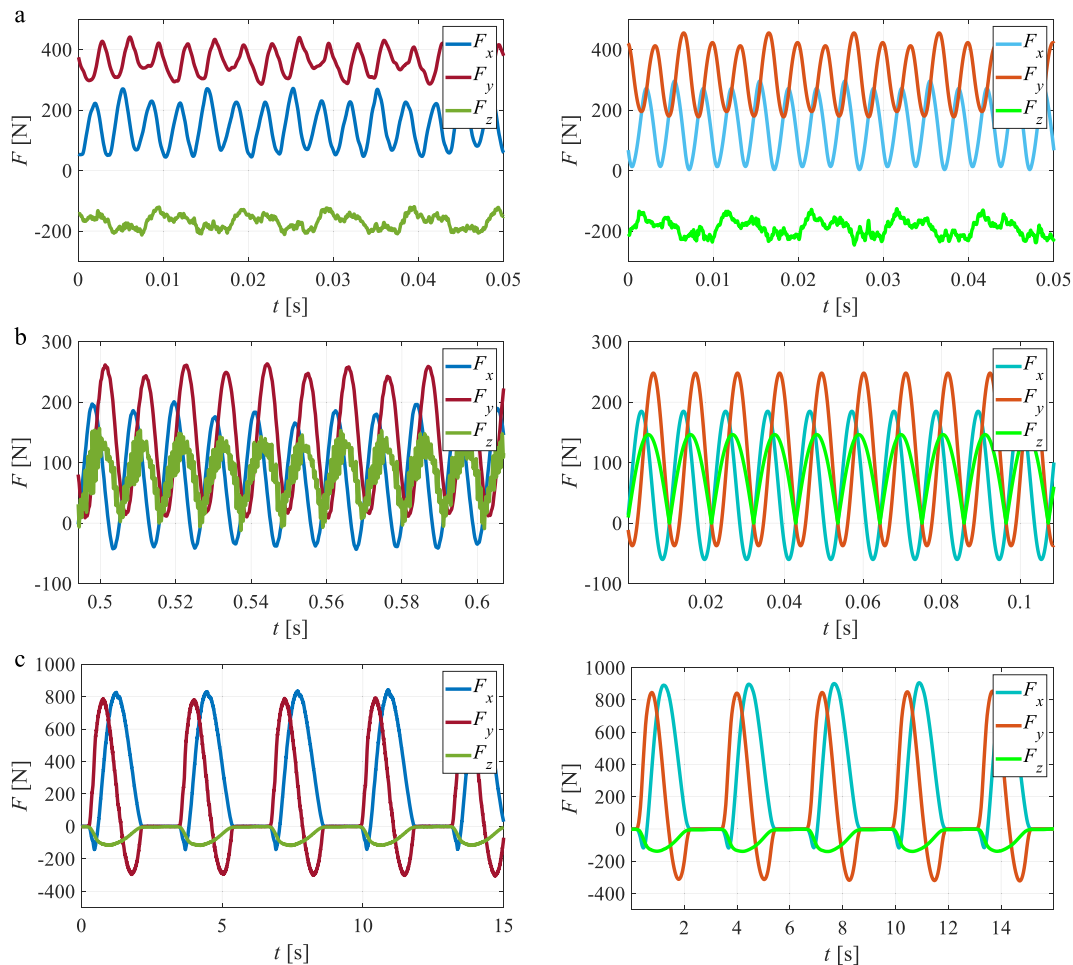
In this case, a power meter (UPC sensor) is installed in the electrical

cabinet to record the power requested by the milling spindle head. A Hall effect sensor was installed on the three phases powering the machine tool's spindle. Fig. 6 shows the measurements of power consumption during machining and idle periods (the latter are taken at the starting or ending of the cutting process).

Table 5 list the parameter process values used for the characterization of the 10 cases in Table 6. The experimentally measured values are used to check the predictions of the proposed model. To obtain the power from using of the model, the idle power ( $P_0$ ) needs to be calibrated for a range of spindle speeds ( $N = 2800\text{--}6631$ ,  $P_0(S) = p_1 \cdot S^2 + p_2 \cdot S + p_3$ ,  $p_1 = 8.259e-09$ ,  $p_2 = -4.69e-05$ ,  $p_3 = 0.5166$ ). Then, the cutting power can be calculated using an expression similar to that presented for instance in [47,48]:

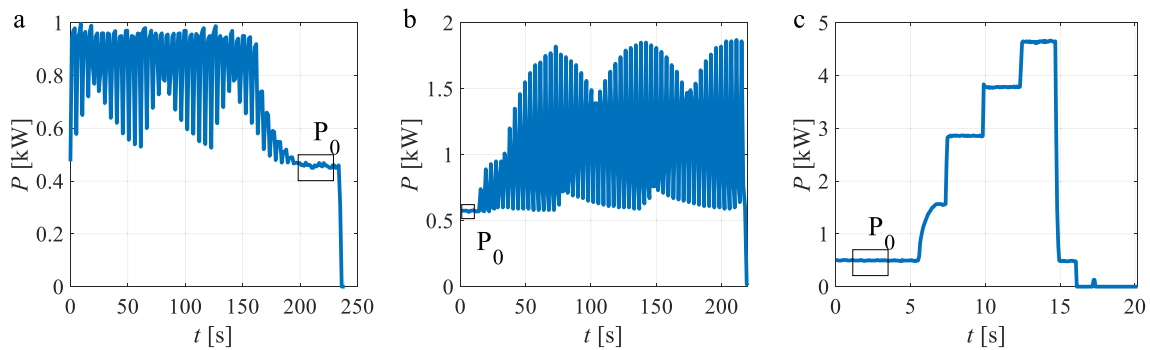
$$P = P_0 + (F_c \cdot V_c / 60) / 10^3 \quad (7)$$

Fig. 7 shows a good correspondence between the calculated cutting power and the measured values. Both share similar trends even if models tend to overestimate the real cutting power. The predicted one is always higher because the experimental one considers also the cut-off transition periods between consecutive radial passes (plunge) or planetary orbits (trochoidal) that tend to diminish the average power. Even for the same

**Fig. 5.** Model validation (left-experimental, right-predicted). a. Serrated milling; b. Plunge milling; c. Trochoidal milling.

**Table 4**  
Tests and cutting conditions (level 2).

Cutting process	Case	$a_p$ [mm]	$a_e$ or $c$ [mm]	$f_z$ [mm/rev/tooth]	$v_f$ [mm/min]	$N$ [rpm]	$V_c$ [m/min]
Plunge milling	1	60	1.25	0.15	840	2800	176
	2		1.30	0.16	896		
	3		1.75	0.20	1120		
	4		1.60	0.18	1008		
	5		1.25	0.175	980		
Trochoidal milling	6	60	0.50	0.05	995	6631	250
	7		0.75	0.10	1989		
	8		0.80	0.06	1194		
	9		0.50	0.10	1989		
	10		0.60	0.08	1591		
Serrated milling	11	10	20	0.05	675	4500	282
	12			0.075	1012		
	13			0.10	1350		
	14	5	20	0.10	1350	4500	282
	15			0.15	2025		
	16			0.20	2700		



**Fig. 6.** Profile of the measured power consumption measured (UPC-E sensor). A. Plunge milling; b. Trochoidal milling; c. Serrated slot milling.

kind of operation, the difference can also be variable from one case to another due to a different number of passes and slopes for the tested cases. If more passes are programmed more cut-off periods are considered. If cut-off periods are minimized the difference between both would be shorter.

## 6. Sustainable productivity gain

The aforementioned levels bring up the opportunity for building more practical parameters: the  $Q_w/P$  ratio (which indeed is dependent on the specific cutting force) and the SPG (Sustainable Productivity Gain), which represent the absolute and relative versions of a concept for stating how efficient one given operation is. Specifically, the second one can be defined as a ratio of ratios:

$$SPG = \frac{i_{Q_w}}{i_P} \quad (8)$$

where  $i_{Q_w} = Q_{w,2}/Q_{w,1}$  and  $i_P = P_2/P_1$  are the chip flow and power consumption ratios for operations #1 and #2. This non-dimensional parameter allows selecting the most effective cutting parameters from both points of view: maximum removal rate at the minimum power consumption.

Table 5 compares both results predicted and experimental data. All the cases were referred to the best case (last Case 16,  $SPG = 1$ ). The highest value here is so  $SPG = 1$ . Some small error are found between modelled and experimentally obtained SPG, mainly due to cutting power calculation. However, the trend is similar for both sets of values. For the tested cutting parameter range, serrated milling is the preferred option, followed by plunge milling. The best compromise between material removal rate and power consumption was found in Case 16 and the worst one in Case 6. Note also that, for the same mass removal rate,

the SPG index recommends Cases 14-15-16 vs. Cases 11-12-13. It is also capable of detecting that Case 13 is more favorable than Case 14.

For the serrated slot milling, Cases 14-15-16 provide equivalent chip flow in comparison with Cases 11-12-13. The SPG index states that Case 14-15-16 are preferable to 11-12-13 because under the same volume of material removed lower power consumption was found.

Neglecting the effect of the cutting speed for the sake of simplicity, the variation of cutting power, chip flow, and the absolute-relative sustainable productivity index can be represented. Fig. 8 shows the surface maps for these functions in the case of the plunge milling process. Clearly, cutting power and chip flow are functions increasing with  $c$  and  $f_z$ , but as they grow differently, it is interesting to read the ratios of their respective evolutions simultaneously. In this sense, Fig. 8c and 8d represent a complete picture of the capabilities of milling operations.

As an optimization criterion, isolines as shown in Fig. 8d can be drawn. These isolines represent equivalent combinations of cutting parameters  $c$ - $f_z$  in terms of productivity and sustainability. So, it can be used by process engineers when it comes to choosing the best cutting conditions for a specific milling operation.

For instance, for a fixed parameter window, i.e.  $c[1-4]$  and  $f_z[0.05-0.30]$ , Fig. 8c and 8d propose margins for improvement in Case 1. The SPG index suggests that  $c = 4$  and  $f_z = 0.175$  mm/Z/rev is the most convenient combination for a productive-sustainable operation. Alternatively, machinists can choose equivalent solutions following the isolines. Then, to minimize power consumption, the minimum value for  $f_z$  (Fig. 8d) can be found. In that case, it seems that it is more convenient increasing the feed rather than the slope between passes.

## 7. Conclusions

This work proposes a methodology to reduce energy consumption in



**Table 5**  
Selecting the maximum productivity – minimum energy process (level 2).

Cases	Experimental values						Modelled values											
	$t$ [s]	$V$ [cm <sup>3</sup> ]	$P_0$ [kW]	$P$ [kW]	$E$ [kJ]	$Q_w$ [cm <sup>3</sup> /s]	$Q_w/P$	SPG	#	$F_x$ [N]	$F_y$ [N]	$F_z$ [N]	$F_t$ [N]	$P$ [kW]	$Q_w$ [cm <sup>3</sup> /s]	$Q_w/P$	SPG	#
1	199.7	55.2	0.45	0.81	162.0	0.276	0.341	0.35	11°	56.2	95.0	84.0	139	0.86	0.277	0.322	0.30	11°
2	157.9	48.4	0.46	0.86	134.9	0.306	0.356	0.37	10°	62.4	105.4	93.1	154	0.91	0.303	0.333	0.31	10°
3	95.6	46.8	0.46	1.02	95.6	0.504	0.494	0.51	7°	105.0	177.3	156.7	259	1.22	0.483	0.396	0.37	7°
4	111.0	50.4	0.46	0.96	105.5	0.459	0.478	0.49	8°	86.4	145.9	129	213	1.09	0.408	0.374	0.35	8°
5	202.3	63.6	0.46	0.86	174.6	0.314	0.365	0.38	9°	65.6	110.8	98	162	0.94	0.312	0.332	0.31	9°
6	171.0	18	0.57	1.09	190.4	0.105	0.096	0.10	16°	140	79	26	160	1.22	0.103	0.084	0.08	16°
7	126.6	40.8	0.58	1.75	231.1	0.322	0.184	0.19	12°	249	155	69	302	1.84	0.313	0.170	0.16	12°
8	142.3	30.0	0.58	1.53	219.2	0.211	0.138	0.14	15°	227	121	43	261	1.66	0.200	0.121	0.11	15°
9	119.0	26.4	0.57	1.42	170.1	0.222	0.156	0.16	13°	174	120	49	217	1.47	0.208	0.142	0.13	13°
10	106.0	21.6	0.56	1.47	155.5	0.204	0.139	0.14	14°	198	118	38	234	1.54	0.200	0.130	0.12	14°
11	2.25	5.06	0.50	3.34	4.38	2.25	0.675	0.70	6°	155	423	242	511	2.90	2.25	0.776	0.73	6°
12	2.25	7.59	0.50	4.41	5.72	3.375	0.765	0.79	5°	192	596	362	723	3.90	3.375	0.865	0.82	4°
13	2.25	10.1	0.50	5.49	7.11	4.5	0.820	0.85	3°	233	757	485	928	4.86	4.5	0.926	0.87	3°
14	2.25	5.06	0.50	2.86	4.11	2.25	0.786	0.81	4°	122	378	212	450	2.62	2.25	0.859	0.81	5°
15	2.25	7.59	0.50	3.78	6.14	3.375	0.893	0.92	2°	155	518	309	623	3.43	3.375	0.984	0.93	2°
16	2.25	10.1	0.50	4.64	7.90	4.5	0.970	1	1°	211	653	404	796	4.24	4.5	1.061	1	1°

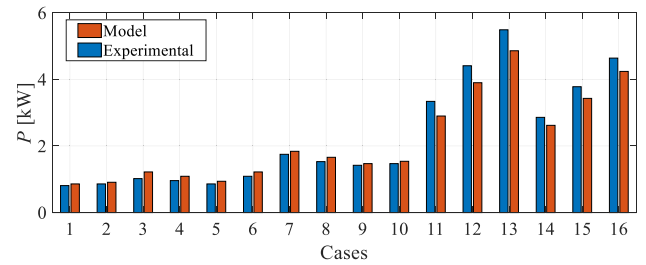


Fig. 7. Power consumption (experimental vs. modelled values).

heavy rough milling operations but considering both productivity and sustainability. The work evaluated and compared three different alternatives -plunge milling, trochoidal milling and serrated milling- for the milling of a depth cavity. The major contributions of the study are:

- Three milling force models were developed by the authors. These models are similar to mechanistic cutting force models in the literature. However, the key point here is the way these models were subsequently derived towards higher stages of knowledge. Key process variables such as force, power and chip flow were validated against experimental values. After their reliability was successfully proven, it is possible to build a quantitative and absolute factor for an operation ad a relative one if comparing two operations. It is important to see that this factor can compare two different kinds of operation such as a set of cutting conditions in plunge milling versus in trochoidal milling. It can be built either through models or experimentally.
- This factor allowed us to determine that, for the studied range, serrated slot milling was the best alternative, followed by plunge and trochoidal milling. However, trochoidal milling could be an interesting alternative process in case of high-quality surface requirements or when tool life should be enhanced. However, aspects such as surface roughness, wear, or vibrations were neglected through this study.
- The proposed approach gives the clue to choose the best milling process in terms of the best use of machine tool's available energy. A methodology based on a new factor, Sustainable Productivity Gain (SPG), is proposed to evaluate how good is one given milling operation versus another. This term allows comparing not only different cutting parameters for a given operation but also different kinds of milling operations with different cutting parameters to state *a priori* which of them is the best option. It is a meaningful index when it comes to comparing milling processes with very different kinematics. Alternatively, the procedure to obtain the Sustainable Productivity Gain can be more easily applied, i.e. without using models, by measuring the cutting power and chip flow parameters.
- The efficiency in milling process was formulated by taking into account power consumption and mass-removal rate. Under this approach, some of the main parameters involved in process planning -i.e. 1) process kinematics; 2) tool-path strategy, 3) cutting parameters- are considered. In terms of work material, this methodology is still valid for different tool-workpiece materials, once that cutting coefficients between tool-workpiece are characterized. The methodology would still be applicable, even with the inherent complications in that cases.
- In this line, future work and models should also include other relevant parameters such as surface roughness, tool wear or modal parameters (dynamic forces). Surface roughness parameter was intentionally left out of this study as it is not a so relevant parameter in rough operations. Nevertheless it would lead to a more complete SPG factor when analyzing finishing operations, milling of difficult to cut materials, etc.

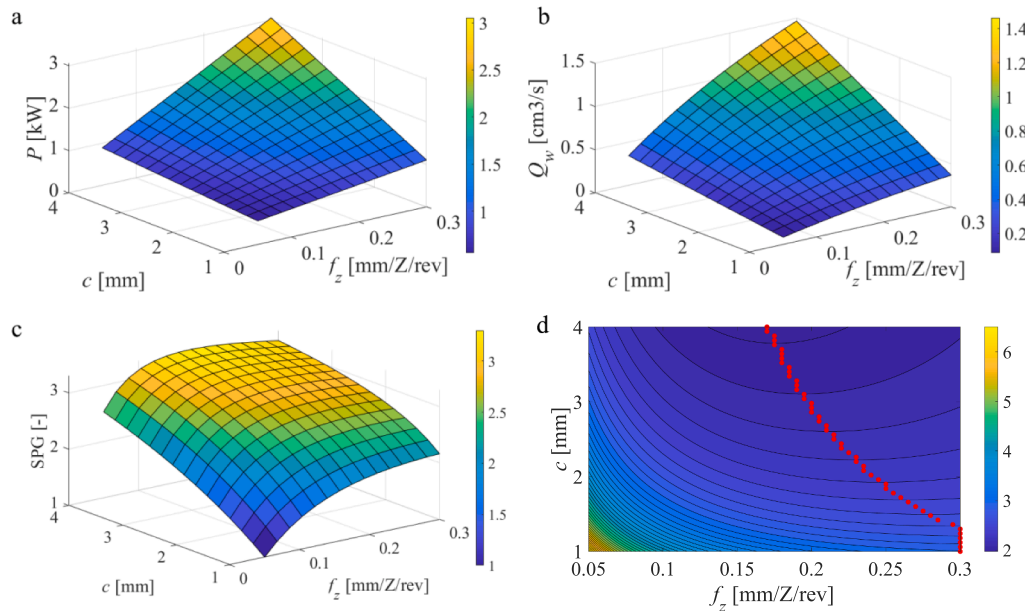


Fig. 8. Effect of cutting parameters for plunge milling (reference Case 1 at minimum  $c$  and  $f_z$ ). a. Cutting power; b. Chip flow; c. SPG (perspective); d. SPG (2D map) with optimization curve overlapped.

#### CRediT authorship contribution statement

**G. Urbikain Pelayo:** Conceptualization, Methodology, Validation, Writing – original draft, Writing – review & editing. **D. Olvera-Trejo:** Methodology, Validation, Writing – original draft, Writing – review & editing. **M. Luo:** Methodology, Writing – review & editing. **K. Tang:** Methodology, Writing – review & editing. **L.N. López Lacalle:** Supervision, Resources. **A. Elías-Zuñiga:** Supervision, Resources.

#### Declaration of Competing Interest

The authors declare that they have no known competing financial interests or personal relationships that could have appeared to influence the work reported in this paper.

#### Acknowledgements

The authors acknowledge the support from the Spanish Government (JANO, CIEN Project, 2019.0760) and Basque Government (ELKAR-TEK19/46, KK-2019/00004).

This research was funded by Tecnológico de Monterrey through the Research Group of Nanotechnology for Devices Design, and by the Consejo Nacional de Ciencia y Tecnología de México (Conacyt), Project Number 296176, and National Lab in Additive Manufacturing, 3D Digitizing and Computed Tomography (MADiT) LN299129.

The authors also acknowledge the support from Garikoitz Goi-koetxea and fruitful discussions with Mr. Jon Méndez (Gühring©) and Endika Monge (Hoffmann Group©).

#### References

- [1] W. Cai, F. Liu, X. Zhou, J. Xie, Fine energy consumption allowance of workpieces in the mechanical manufacturing industry, *Energy* 114 (2016) 623–633.
- [2] D.A. Marcontell, Engine MRO market: An overview of the current State of the Aero-Engine Fleet, Oliver Wyman-Aviation, Aerospace & Defense, 2016.
- [3] F.I. Compeán, D. Olvera, F.J. Campa, L.N. López de Lacalle, A.E. Zúñiga, C. A. Rodríguez, Characterization and stability analysis of a multivariable milling tool by the enhanced multistage homotopy perturbation method, *Int. J. Mach. Tools Manuf* 57 (2012) 27–33.
- [4] A. Comak, E. Budak, Modeling dynamics and stability of variable pitch and helix milling tools for development of a design method to maximize chatter stability, *Precis. Eng.* 47 (2017) 459–468.
- [5] J. Niu, Y. Ding, L.M. Zhu, H. Ding, Mechanics and multi-regenerative stability of variable pitch and variable helix milling tools considering runout, *Int. J. Mach. Tools Manuf* 123 (2017) 129–145.
- [6] R. Koca, E. Budak, Optimization of serrated end mills for reduced cutting energy and higher stability, *Procedia CIRP* 8 (2013) 570–575.
- [7] R. Grabowski, B. Denkena, J. Kohler, Prediction of process forces and stability of end mills with complex geometries, *Procedia CIRP* 14 (2014) 119–124.
- [8] F. Tehranizadeh, R. Koca, E. Budak, Investigating effects of serration geometry on milling forces and chatter stability for their optimal selection, *Int. J. Mach. Tools Manuf* 144 (2019).
- [9] G. Urbikain, D. Olvera, Model-based phase shift optimization of serrated end mills: Minimizing forces and surface location error. *Mechanical Systems and Signal Processing* 144, 2020.
- [10] J.H. Ko, Y. Altintas, Time domain model of plunge milling operation, *Int. J. Mach. Tools Manuf* 47 (2007) 1351–1361.
- [11] K. Zhuang, X. Zhang, D. Zhang, H. Ding, On cutting parameters selection for plunge milling of heat-resistant-super-alloys based on precise cutting geometry, *J. Mater. Process. Technol.* 213 (8) (2013) 1378–1386.
- [12] X.Y. Yang, J.Y. Tang, Research on manufacturing method of CNC plunge milling for spur face-gear, *J. Mater. Process. Technol.* 214 (12) (2014) 3013–3019.
- [13] F.Y. Han, D.H. Zhang, M. Luo, B.H. Wu, Optimal CNC plunge cutter selection and tool path generation for multi-axis roughing free-form surface impeller channel, *Int. J. Adv. Manuf. Technol.* 71 (9–12) (2014) 1801–1810.
- [14] S. Cafieri, F. Monies, M. Mongeau, C. Bes, Plunge milling time optimization via mixed-integer nonlinear programming, *Comput. Ind. Eng.* 98 (2016) 434–445.
- [15] M. Otkur, I. Lazoglu, Trochoidal milling, *Int. J. Mach. Tools Manuf* 47 (9) (2007) 1324–1332.
- [16] S. Wu, W. Ma, B. Li, C. Wang, Trochoidal machining for the high-speed milling of pockets, *J. Mater. Process. Technol.* 233 (2016) 29–43.
- [17] A. Pleta, G. Nithyanand, F.A. Niaki, L. Mears, Identification of optimal machining parameters in trochoidal milling of Inconel 718 for minimal force and tool wear and investigation of corresponding effects on machining affected zone depth, *J. Manufact. Processes* 43(Part B) (2019) 54–62.
- [18] M. Luo, C. Hah, H.M. Hafeez, Four-axis trochoidal toolpath planning for rough milling of aero-engine blisks, *Chin. J. Aeronaut.* 32 (8) (2019) 2009–2016.
- [19] Z. Li, L. Chen, K. Xu, Y. Gao, K. Tang, Five-axis trochoidal flank milling of deep 3D cavities, *Comput. Aided Des.* (2020) 119.
- [20] O.I. Avram, P. Xirouchakis, Evaluating the use phase energy requirements of a machine tool system, *J. Cleaner Prod.* 19 (6–7) (2011) 699–711.
- [21] V.A. Balogun, P.T. Mativenga, Modelling of direct energy requirements in mechanical machining processes, *J. Cleaner Prod.* 41 (2013) 179–186.
- [22] M.P. Sealy, Z.Y. Liu, Y.B. Guo, Z.Q. Liu, Energy based process signature for surface integrity in hard milling, *J. Mater. Process. Technol.* 238 (2016) 284–289.
- [23] F. Ma, H. Zhang, H. Cao, K.K.B. Hon, An energy consumption optimization strategy for CNC milling, *Int. J. Adv. Manuf. Technol.* 90 (2017) 1715–1726.
- [24] K. Xu, M. Luo, K. Tang, Machine based energy-saving tool path generation for five-axis end milling of freeform surfaces, *J. Cleaner Prod.* 139 (2016) 1207–1223.
- [25] Lv et al., J. Lv, R. Tang, W. Tang, Y. Liu, Y. Zhang, S. Jia, An investigation into reducing the spindle acceleration energy consumption of machine tools, *J. Clean. Product.* 143 (2017) 794–803.

- [26] S.-J. Shin, J. Woo, S. Rachuri, Energy efficiency of milling machining: component modeling and online optimization of cutting parameters, *J. Cleaner Prod.* 161 (2017) 12–29.
- [27] S. Wojciechowski, R.W. Maruda, S. Barrans, P. Nieslony, G.M. Krolczyk, Optimisation of machining parameters during ball end milling of hardened steel with various surface inclinations, *Measurement* 111 (2017) 18–28.
- [28] Y. Cai, X. Shi, H. Shao, R. Wang, S. Liao, Energy efficiency state identification in milling processes based on information reasoning and Hidden Markov Model, *J. Cleaner Prod.* 193 (2018) 397–413.
- [29] Y. Cai, X. Shi, H. Shao, J. Yuan, Energy efficiency state identification based on continuous wavelet transform-fast independent component analysis, *J. Manufact. Sci. Eng.* 141 (2) (2019), 021012.
- [30] K.N. Shi, D.H. Zhang, N. Liu, S.B. Wang, J.X. Ren, S.L. Wang, A novel energy consumption model for milling process considering tool wear progression, *J. Cleaner Prod.* 184 (2018) 152–159.
- [31] K.N. Shi, J.X. Ren, S.B. Wang, N. Liu, Z.M. Liu, D.H. Zhang, W.F. Lu, An improved cutting power-based model for evaluating total energy consumption in general end milling process, *J. Cleaner Prod.* 231 (2019) 1330–1341.
- [32] K. Venkata Rao, Power consumption optimization strategy in micro ball-end milling of D2 steel via TLBO coupled with 3D FEM simulation, *Measurement* 132 (2018) 68–78.
- [33] T. Zhang, Z. Liu, X. Sun, J. Xu, L. Dong, G. Zhu, Investigation on specific milling energy and energy efficiency in high-speed milling based on energy flow theory, *Energy* 192 (1) (2020), 116596. February 2020.
- [34] J. Yuan, H. Shao, Y. Cai, X. Shi, Energy efficiency state identification of milling processing based on EEMD-PCA-ICA, *Measurement* 174 (2021) 109014.
- [35] T.T. Nguyen, Prediction and optimization of machining energy, surface roughness, and production rate in SKD61 milling, *Measurement* 136 (2019) 525–544.
- [36] P.M. Gopal, K.S. Prakash, Minimization of cutting force, temperature and surface roughness through GRA, TOPSIS and Taguchi techniques in end milling of Mg hybrid MMC, *Measurement* 116 (2018) 178–192.
- [37] K. Venkata Rao, Power consumption optimization strategy in micro ball-end milling of D2 steel via TLBO coupled with 3D FEM simulation, *Measurement* 132 (2019) 68–78.
- [38] S. Wojciechowski, M. Wiackiewicz, G.M. Krolczyk, Study on metrological relations between instant tool displacements and surface roughness during precise ball end milling, *Measurement* 129 (2018) 686–694.
- [39] K. Klauer, M. Eifler, B. Kirsch, J. Seewig, J.C. Aurich, Ball end micro milling of areal material measures: influence of the tilt angle on the resulting surface topography, *Prod. Eng. Res. Devel.* 14 (2020) 239–252.
- [40] J. Zhang, S. Zhang, D. Jiang, J. Wang, S. Lu, Surface topography model with considering corner radius and diameter of ball-nose end miller, *Int. J. Adv. Manuf. Technol.* 106 (2020) 3975–3984.
- [41] G. Urbikain, D. Olvera-Trejo, m. Luo, L.N. López de Lacalle, A. Elfas-Zúñiga, Surface roughness prediction with new barrel-shape mills considering runout: modelling and validation, *Measurement* 173 (2021) 108670.
- [42] G. Urbikain, Modelling of static and dynamic milling forces in inclined operations with circle-segment end mills, *Precis. Eng.* 56 (2019) 123–135.
- [43] Z. Yao, M. Luo, J. Mei, D. Zhang, Position dependent vibration evaluation in milling of thin-walled part based on single-point monitoring, *Measurement* 171 (2021) 108810.
- [44] S.Q. Wang, C.L. He, J.G. Li, J. Wang, Vibration-free surface finish in the milling of a thin-walled cavity part using a corn starch suspension, *J. Mater. Process. Technol.* 290 (2021) 116980.
- [45] S. Cai, Z. Cai, B. Yao, Z. Shen, X. Ma, Identifying the transient milling force coefficient of a slender end-milling cutter with vibrations, *J. Manuf. Processes* 67 (2021) 262–274.
- [46] B. Toubhans, G. Fromentin, F. Viprey, H. Karaoui, T. Dorlin, Machinability of inconel 718 during turning: Cutting force model considering tool wear, influence on surface integrity, *J. Mater. Process. Technol.* 285 (2020) 116809.
- [47] T. Gutowski, J. Dahmus., A. Thiriez, Electrical energy requirements for manufacturing processes, in: 13th CIRP international conference on life cycle engineering, Volume 31, 1, Leuven, Belgium, 2006.
- [48] V. Astakhov, x. Xiao, Cutting Force Evaluation Based On Total Energy Consumption, SAE International, 2008.